Aharonov-Bohm Oscillations in Singly Connected Disordered Conductors

I. L. Aleiner,[1] A. V. Andreev,[2] and V. Vinokur[3]
[1]Department of Physics, Columbia University, New York, New York 10027, USA
[2]Department of Physics, University of Washington, Seattle, Washington 98195, USA
[3]Materials Science Division, Argonne National Laboratory, Argonne, Illinois 60439, USA
(Received 20 December 2014; published 20 February 2015)

We show that the transport and thermodynamic properties of a *singly connected* disordered conductor exhibit quantum Aharonov-Bohm oscillations as a function of the total magnetic flux through the sample. The oscillations are associated with the interference contribution from a special class of electron trajectories confined to the surface of the sample.

DOI: 10.1103/PhysRevLett.114.076802 PACS numbers: 73.23.-b, 74.78.-w, 74.78.Na

Introduction.—Quantum coherence of electron motion dramatically affects low temperature phenomena in disordered conductors. Anderson localization [1] is the most profound of them, but even in the metallic regime, where quantum effects are relatively small, they give rise to a number of dramatic effects due to their extreme sensitivity to magnetic field and inelastic processes [2,3]. Celebrated examples are universal conductance fluctuations (UCF) [4,5], magnetoresistance in weak magnetic fields [6], and Aharonov-Bohm (AB) oscillations [7] in thin mesoscopic cylinders and rings [8,9]. Here we show that quantum interference corrections give rise to a novel type of AB oscillations that exist in finite *singly connected* conductors. They originate from the boundary of the sample and are associated with a special type of diffusive trajectories that graze the boundary.

In the metallic regime quantum corrections may be understood semiclassically. One can start with the classical motion of electrons with momentum $\mathbf{p}$, where $|\mathbf{p}| \simeq p_F$ (p_F is the Fermi momentum) along diffusive trajectories ("paths") consisting of segments of straight lines broken by impurities, [see Fig. 1(a)]. The phase θ_l of the quantum amplitude for the lth path is

$$\theta_l(\mathbf{B}) = \frac{p_F L_l}{\hbar} + \frac{e}{c\hbar}\int_l d\mathbf{r}\cdot\mathbf{A}. \tag{1}$$

Here, L_l is the path length and the second term is the Aharonov-Bohm phase due to the magnetic field, $\mathbf{B} = \nabla \times \mathbf{A}$. Observables may be expressed in terms of the sum of quantum amplitudes taken over all classical paths connecting two points ($\mathbf{r}_1$ and $\mathbf{r}_2$ in Fig. 1), i.e.,

$$\left|\sum\nolimits_l \sqrt{W_l}\, e^{i\theta_l}\right|^2 = \sum_l W_l + 2\mathrm{Re}\sum_{l\neq l'} \sqrt{W_l W_{l'}}\, e^{i(\theta_l-\theta_{l'})}, \tag{2}$$

where W_l is the classical probability of path l. The first sum on the right-hand side of Eq. (2) corresponds to the classical probability of propagation from $\mathbf{r}_1$ to $\mathbf{r}_2$. The second gives the quantum correction that arises from interference of amplitudes of different trajectories, and is in general random due to rapidly oscillating phase factors. Consideration of leading quantum corrections amounts to statistical analysis of these random terms. For example, the weak localization correction is determined by its average whereas UCF are determined by its second cumulant.

One of the main objects governing the statistics of quantum corrections [2] is the *Cooperon*. It describes interference of pairs of geometrically identical paths traversed in opposite directions,

$$C(\mathbf{r}_1,\mathbf{r}_2;\mathbf{B}) = \sum_l W_l e^{i[\theta_l(\mathbf{B})-\theta_l(-\mathbf{B})]}. \tag{3}$$

In the absence of magnetic field the phase factors above are equal to unity, and the Cooperon is given by the probability

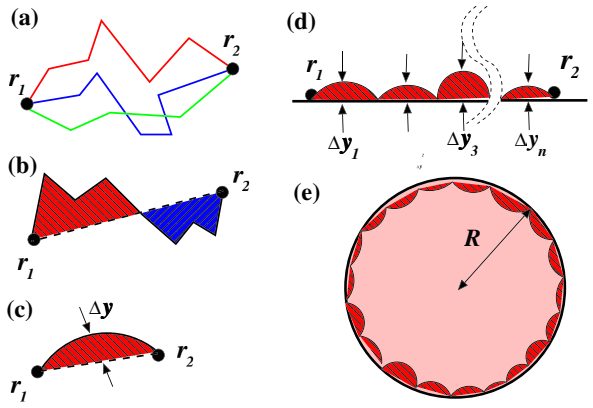

FIG. 1 (color online). (a) Diffusive paths contributing to the interference corrections. (b) Sketch of the directed area swept by a path. The blue and red regions give opposite in sign contributions. (c) Typical path leading to the Gaussian decay of the Cooperon in the bulk. (d) Typical path near the surface. (e) Surface paths leading to AB oscillations. Notice that the straight segment structure of diffusive paths in (a),(b) is not shown in panels (c)–(e).

of classical diffusion between points $\mathbf{r}_1$, $\mathbf{r}_2$. In a finite magnetic field the phase factors become random due to accumulation of Aharonov-Bohm flux through oriented areas swept by diffusive paths [see Fig. 1(b)]. It is well known [2] that this randomness suppresses the Cooperon at distances larger than the magnetic length, $l_B = \sqrt{\hbar c/eB}$, so that for an infinite system $C(\mathbf{r}_1, \mathbf{r}_2; \mathbf{B}) \simeq \exp[2ie/(\hbar c) \int \mathbf{A} \cdot d\mathbf{r} - \alpha_b(\mathbf{r}_1 - \mathbf{r}_2)^2/l_B^2]$, where α_b is a constant of order unity and the integral is taken along the chord connecting $\mathbf{r}_1$ and $\mathbf{r}_2$.

As will be shown below, directed areas swept by electron trajectories near the boundary have smaller randomness than those in the bulk. As a result, near the boundary the Cooperon has a very different coordinate dependence from that in the bulk; $C(\mathbf{r}_1, \mathbf{r}_2; \mathbf{B}) \simeq \exp[\int_s (2ie/(\hbar c)\mathbf{A} \cdot d\mathbf{r} - \alpha_s |d\mathbf{r}|/l_B)]$. Here α_s is a constant of order unity, and the integration is taken along the boundary. In contrast to the Gaussian falloff of the bulk contribution with distance $r_{12} \equiv |\mathbf{r}_1 - \mathbf{r}_2|$, the surface contribution falls off exponentially and thus becomes dominant at large distances. Another important distinction is that the Aharonov-Bohm phase of the surface contribution is determined by the geometry of the *sample* boundary rather than the shortest line connecting the end points. Furthermore, the requirement that on completing the perimeter of the sample; see Fig. 1(e), the Cooperon must remain unchanged means that the surface contribution $C(\mathbf{r}, \mathbf{r}; \mathbf{B})$ is, in fact, an oscillating function of the magnetic flux through the sample, Φ, $C(\mathbf{r}, \mathbf{r}; \mathbf{B}) \simeq \cdots + \exp(-\alpha_s p/l_B) \cos(2\pi\Phi/\Phi_0)$, where $\Phi_0 = 2\pi\hbar c/2e$ is the superconducting flux quantum and p is the length of the perimeter (for a three-dimensional system p and Φ are, respectively, the perimeter of the extremal cross section perpendicular to the magnetic field, and the flux through it). This means that the quantum interference corrections are expected to *oscillate* (rather than simply decay) with the magnetic field even in singly connected geometries [10], in a way similar to the effects in multiple connected geometries [7,8,11].

Qualitative discussion.—To elucidate the difference between the surface and the bulk contributions to the interference corrections we now discuss the statistics of diffusive trajectories in more detail. Let us label each diffusive trajectory by $\mathbf{r}(\tau)$, $0 \le \tau \le t$, where t is the duration of the diffusive motion. Then summation over the paths l can be rewritten as

$$\sum_l W_l \to \int dt P(t); \quad P(t) \simeq \sum_{\mathbf{r}(\tau)} \exp\left(-\frac{\int_0^t d\tau \dot{\mathbf{r}}^2}{4D}\right),$$

where D is the diffusion constant, and the summation (path integration) is performed over all trajectories $\mathbf{r}(\tau)$ in which the particle travels from $\mathbf{r}_1$ to $\mathbf{r}_2$ in time t. In this notation the bulk contribution to the Cooperon (3) acquires the form

$$C(\mathbf{r}_1, \mathbf{r}_2; \mathbf{B}) = e^{i\theta^{\mathrm{AB}}_{\mathbf{r}_1\mathbf{r}_2}} \int dt P(t) \left\langle \exp\left(\frac{2iS\{\mathbf{r}(t)\}}{l_B^2}\right) \right\rangle, \quad (4)$$

where the Aharonov-Bohm phase $\theta^{\mathrm{AB}}_{\mathbf{r}_1\mathbf{r}_2} = (i2e/\hbar c) \int_{\mathbf{r}_1}^{\mathbf{r}_2} d\mathbf{r} \cdot \mathbf{A}$ is calculated along the straight line connecting points $\mathbf{r}_1$ and $\mathbf{r}_2$, $S\{\mathbf{r}(t)\}$ is the directed area of the surface confined by the path $\mathbf{r}(t)$ and the straight line connecting points $\mathbf{r}_1$, $\mathbf{r}_2$, see Fig. 1, and the averaging means

$$\langle \ldots \rangle = \frac{1}{P(t)} \sum_{\mathbf{r}(\tau)} \ldots \exp\left(-\frac{1}{4D} \int_0^t d\tau \dot{\mathbf{r}}^2\right). \quad (5)$$

Some conclusions about the statistical properties of S can easily be drawn on symmetry and dimensionality grounds. Consider, for example, a typical diffusive path shown in Fig. 1(c). Its probability can be estimated as $\exp[-(r_{12}^2 + (\Delta y)^2)/(4Dt)]$ while the directed area swept by it is $S \simeq 1/2 |r_{12}| \Delta y$. Then, the averaged phase factor is given by

$$\left\langle \exp\left(\frac{2iS}{l_B^2}\right) \right\rangle \propto \int_{-\infty}^{\infty} d\Delta y \exp\left(\frac{i r_{12} \Delta y}{l_B^2}\right) \exp\left(-\frac{(\Delta y)^2}{4Dt}\right) \propto \exp(-Dt r_{12}^2/l_B^4) \quad (6)$$

(the prefactor is easily found from the $l_B \to \infty$ limit). Substituting this estimate into Eq. (4), we obtain

$$C(\mathbf{r}_1, \mathbf{r}_2; \mathbf{B}) \simeq \int dt \exp[-\mathbf{r}_{12}^2/(4Dt)] \exp(-Dt r_{12}^2/l_B^4).$$

The exponent in the integrand has a minimum at $Dt \simeq l_B^2$ and at $|r_{12}| \gg l_B$ can be evaluated in the saddle point approximation with the result that in the *interior* of the system the Cooperon decays rapidly at large distances,

$$|C(\mathbf{r}_1, \mathbf{r}_2; \mathbf{B})| \propto \exp(-r_{12}^2/l_B^2). \quad (7)$$

This rapid spatial decay of the bulk contribution arises from an *unconstrained* summation of a large number of contributions in (6), which have random signs and nearly cancel each other. The presence of a nearby boundary imposes a sharp geometrical constraint on the allowed paths, which enhances the sum of rapidly oscillating contributions of different paths. For instance, consider the same trajectory as in Fig. 1(c), but for both points $\mathbf{r}_1$ and $\mathbf{r}_2$ near the boundary. For such trajectories the geometric constraint imposed by the boundary amounts to confining the integration variable y to the interval $y \in [0, \infty)$ resulting in a contribution of the form

$$\left| \int_0^{\infty} dy \exp\left(\frac{i r_{12} \Delta y}{l_B^2}\right) \exp\left(-\frac{(\Delta y)^2}{4Dt}\right) \right| \simeq \frac{l_b^2}{|r_{12}| \sqrt{Dt}}.$$

Although this contribution decays merely as a power law at $\mathbf{r}_{12} \gg l_B$, there are other oscillatory contributions, which together lead to an exponential decay. Consider a trajectory having the form of the "skipping orbit" shown in Fig. 1(d), which includes n reflections from the boundary. Its probability is $\exp\left(-r_{12}^2/(4Dt) - n\sum_{j=1}^{n}(\Delta y_j)^2/(4Dt)\right)$, while the directed area swept by it is $S \simeq 1/(2n)|r_{12}|\sum_{j=1}^{n}\Delta y_j$. The estimate (6), thus, immediately changes to

$$\left\langle \exp\left(\frac{2iS}{l_B^2}\right)\right\rangle \propto \prod_{j=1}^{n}\int_0^\infty d\Delta y_j \exp\left(\frac{ir_{12}\Delta y_j}{nl_B^2} - n\frac{(\Delta y_j)^2}{4Dt}\right).$$

Estimating n from the requirement that the contribution from both terms in the exponent be of the same order for the relevant value of Δy_j, we find the optimal value of n to be given by $n_*^3 \simeq (tDr_{12}^2)/l_B^4$. The final value of the averaged phase factor becomes

$$\left\langle \exp\left(\frac{2iS}{l_B^2}\right)\right\rangle = (e^{-\alpha_s})^{n_*} = \exp\left[-\alpha_s\left(\frac{tDr_{12}^2}{l_B^4}\right)^{1/3}\right],$$

where α_s is a coefficient of order unity and $\mathrm{Re}\,\alpha_s > 0$. Substituting this estimate into Eq. (4), we find

$$C(\ldots) \simeq \int dt \exp\left[-r_{12}^2/(4Dt)\right]\exp\left[-\alpha_s(tDr_{12}^2/l_B^4)^{1/3}\right].$$

The exponent in the integrand has a minimum at $Dt \simeq l_B r_{12}$ and at $|r_{12}| \gg l_B$ we obtain the main qualitative result,

$$|C_s(\mathbf{r}_1, \mathbf{r}_2; \mathbf{B})| \propto \exp\left(-\alpha_s|r_{12}|/l_B\right), \tag{8}$$

which decays significantly more slowly than in the bulk; see Eq. (7). A similar enhancement of electron tunneling due to the surface effects was pointed out in Ref. [12] in the context of hopping transport in strong magnetic fields. The similarity is only formal, as we consider here the case of a classically weak magnetic field which does not bend the diffusive trajectories of electrons and enters only through the accumulation of the Aharonov-Bohm phase.

Quantitative analysis of the Cooperon.—The qualitative picture above is borne out by quantitative analysis. The Cooperon represents the resolvent of the modified diffusion equation [2],

$$\hbar D[-i\nabla - (2e/\hbar c)\mathbf{A}(\mathbf{r})]^2\chi_\beta(\mathbf{r}) = \epsilon_\beta\chi_\beta(\mathbf{r}), \tag{9a}$$

$$\mathbf{n}\cdot[-i\nabla - (2e/\hbar c)\mathbf{A}(\mathbf{r})]\chi_\beta(\mathbf{r})|_{\mathbf{r}\in\mathcal{B}} = 0. \tag{9b}$$

In the boundary condition (9b) $\mathbf{n}$ is a vector normal to the boundary $\mathcal{B}$. The vector potential $\mathbf{A}$ describes the effect of the Aharonov-Bohm phase accumulation and the boundary condition corresponds to the absence of current through the boundary. The eigenvalues ϵ_β are gauge invariant and in many cases (see below) the physical effects are determined only by them. The Cooperon (3) can be easily expressed as $C(\mathbf{r}_1, \mathbf{r}_2) = \sum_\beta \chi_\beta(\mathbf{r}_1)\chi_\beta^*(\mathbf{r}_2)/\epsilon_\beta$.

To investigate the surface contribution to Aharonov-Bohm oscillations in a singly connected sample it is sufficient to use the simplest disk geometry shown on Fig. 1(e). Equations (9) are easily solved in the polar coordinates r, φ in the symmetric gauge $A_r = 0$, $A_\varphi = -(rB/2)$. The eigenstates in this case are labeled by two integers $\beta \to (n, m)$, where m is the angular momentum, and $n \geq 0$ is the radial number. The wave functions are of the form $\chi = e^{im\varphi}f_m^n(r/l_B)$. The eigenvalue $\epsilon_m^n = \lambda_m^n \hbar D/l_B^2$, and the radial wave function $f_m^n(\rho)$ ($\rho = r/l_B$) obey the dimensionless differential equation

$$\left[-\frac{d^2}{d\rho^2} - \frac{1}{\rho}\frac{d}{d\rho} - 2m + \frac{m^2}{\rho^2} + \rho^2\right] f_m^n(\rho) = \lambda_m^n f_m^n(\rho). \tag{10}$$

The Neumann boundary condition $(df_m^n/d\rho)|_{\rho=R/l_B} = 0$ makes this problem different from that for an electron in a magnetic field. The solution of Eq. (10) that is regular at $\rho = 0$ may be expressed in terms of the confluent hypergeometric function $\Phi(\alpha, \beta, z)$,

$$f_m^n(\rho) = e^{-\rho^2/2}\rho^{|m|}\Phi\left(\frac{|m|+1-m}{2} - \frac{\lambda_m^n}{4}, |m|+1, \rho^2\right).$$

The eigenvalues λ_m^n are found from the boundary condition at $\rho = R/l_B$. For small angular momenta, $m \ll R/l_B$, they correspond to degenerate Landau levels, $\lambda_m^n = 4n + 2$. Near the boundary they show significant deviations. For the two lowest Landau levels λ_m^n are plotted in Fig. 2 for $\Phi/\Phi_0 = 25$.

As shown below, the magnitude of the Aharonov-Bohm oscillations is governed by the spectrum in the vicinity of the lower boundary, $\lambda^* = \min_m \lambda_m^0 \approx 1.18$, which is

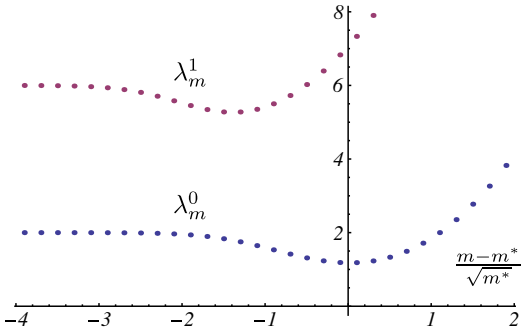

FIG. 2 (color online). Cooperon eigenvalues calculated for a disk geometry. The drop near $m = m^*$ corresponds to the interference of diffusion trajectories near the boundary shown in Fig. 1.

achieved at $m = m^* \approx \Phi/\Phi_0$. Near the minimum the spectrum may be approximated as

$$\lambda_0(m) \equiv \lambda_m^0 \approx \lambda^* \left(1 + \frac{(m-m^*)^2}{\kappa^2 m^*}\right); \quad m^* \approx \frac{\Phi}{\Phi_0} \gg 1, \qquad (11)$$

where $\kappa \approx 1.4$.

To make a connection with the boundary contribution to the Cooperon, Eq. (8), we analyze the asymptotic behavior of the exact expression

$$C(\mathbf{r}, \mathbf{r}') = \sum_{mn} \frac{e^{im(\varphi-\varphi')} f_m^n(r/l_B) f_m^n(r'/l_B)}{\epsilon_m^n}.$$

At large distances, $|\varphi - \varphi'| m^* \gg 1$ and $r \simeq r' \simeq m^* l_B$, the exponential decay is determined by the pole closest to the real axis, and we obtain

$$C \simeq \exp\left[im^*(\varphi - \varphi') - \kappa\sqrt{m^*}|\varphi - \varphi'|\right],$$

which corresponds to the edge physics discussed above.

Physical manifestations.—The surface contribution to the Cooperon gives rise to anomalous magnetic field dependence of the well-known quantum interference corrections to thermodynamic and transport characteristics of disordered conductors. To be concrete, we consider the simplest fluctuation correction to the thermodynamics of the superconductor in the normal state. The surface contribution becomes especially pronounced in the vicinity of the critical field H_{c3} [13]. The fluctuation correction to the free energy, which may be probed in high precision persistent current measurements (see Ref. [14] and references therein), is connected to the eigenvalues (10) by [2]

$$\delta F = T \sum_{k,n,m} \ln\left[\ln\left(\frac{T}{T_{c0}}\right) + \Psi\left(\frac{|k|}{2} + \frac{\hbar D \lambda_m^n}{4\pi l_B^2 T}\right)\right], \qquad (12)$$

where $\Psi(x) \equiv \psi(x + 1/2) - \psi(1/2)$, $\psi(x)$ being the digamma function. The $k = 0$ Matsubara frequency corresponds to the classical fluctuations. Quantum fluctuations are encoded in the summation over all k.

At zero magnetic field $\min \epsilon_\beta = 0$ and the correction (12) is meaningful only for $T > T_{c0}$, where the normal phase is stable. At a finite magnetic field $\lambda_m^n \geq \lambda_* > 0$, and the normal phase is stable even at $T < T_{c0}$ for $B > H_{c3}(T)$, where surface superconductivity emerges [13],

$$\ln(T_{c0}/T) = \Psi(\lambda^* e D H_{c3}(T)/[4\pi c T]). \qquad (13)$$

The part of the free energy oscillating with the total flux Φ can easily be found using Eqs. (10)–(12). Summing over m with the aid of the Poisson summation formula, we obtain to leading exponential accuracy

$$F_{os} = T \sum_{k, j\neq 0} \int_{-1/2}^{\infty} dm e^{i2\pi jm} \times \ln\left[\ln\left(\frac{T}{T_{c0}}\right) + \Psi\left(\frac{|k|}{2} + \frac{\lambda_0(m) e D B}{4\pi c T}\right)\right]. \qquad (14)$$

At $m^* \gg 1$ the integral is determined by the branch cut of the logarithm. The branching point m_b is determined by $\lambda_0(m_b) = \lambda^* H_{c3}/B - 2\pi c T|k|/(eDB)$. Near H_{c3} this condition can be simplified using Eqs. (11) and (13),

$$m_b = m^* \pm i\kappa\sqrt{m^*}\sqrt{\frac{B - H_{c3}(T)}{B} + \frac{2e^\gamma |k| T}{T_{c0}} \frac{H_{c3}(0)}{B}},$$

where $\gamma \approx 0.577$ is the Euler-Mascheroni constant. Integrating along the branch cut and summing over the Matsubara frequencies k, we obtain

$$F = -T \sum_{j=1}^{\infty} \frac{2}{j} \cos\left(\frac{2\pi j \Phi}{\Phi_0}\right) \exp\left(-j\frac{p}{\xi_3}\right) \times \coth\left(j \frac{p}{\xi_3} \frac{e^\gamma T H_{c3}(0)}{2T_{c0}[B - H_{c3}(T)]}\right). \qquad (15)$$

Here the correlation length ξ_3 is determined by the proximity of the magnetic field to the value of $H_{c3}(T)$,

$$\xi_3 = \frac{l_B}{\kappa}\sqrt{\frac{B}{B - H_{c3}}},$$

and $p = 2\pi R$ is the sample perimeter. To arrive at Eq. (15) we used the relation $\sqrt{m^*} = p/(2\pi l_B)$. In this form Eq. (15) remains valid for samples of noncircular shape. The function $\coth x$ in (15) describes the crossover between the classical (at $x \gg 1$) and quantum (at $x \ll 1$) fluctuation regimes. In contrast to a bulk system, the characteristic crossover scale depends on the boundary length, which reflects the surface origin of the effect.

Equation (15) is the main illustrative result for the surface interference contribution we discussed. Similar oscillations should also appear not in the transport properties of mesoscopic singly connected devices, e.g., the Aslamazov-Larkin corrections to the conductance [15] of normal systems or superconductor–normal metal hybrid structures, resembling the results [16] for thin cylinders. Quantitative investigation of transport effects requires analysis of current redistribution near the edges of the sample and will be reported elsewhere. Oscillatory flux dependence of the conductance of singly connected wires and SNS junctions was recently reported in Refs. [17–20]. The observations of Ref. [19] were interpreted in Ref. [21] in terms of formation of superconducting vortices inside the sample. Our findings show that oscillatory flux dependence of the properties of diffusive singly connected conductors is

a much more general phenomenon which occurs even in the absence of superconductivity.

In conclusion, we identified a novel contribution to the magnetic field dependence of quantum interaction corrections in finite conductors. It arises from diffusive trajectories confined to the surface of the sample and gives rise to Aharonov-Bohm oscillations even in singly connected samples. In nonsingly connected samples or samples with holes or cavities, AB oscillations will have multiple periods determined by the areas of extremal sections for each bounding surface.

We thank B. Spivak and D. Cobden for useful discussions and comments on the manuscript. I. A. was supported by the Simons Foundation. A. A. was supported by the U.S. Department of Energy by the Grant No. DE-FG02-07ER46452 and partly supported at ANL by the Materials Theory Institute. V. V. was supported by the U.S. Department of Energy, Office of Science, Materials Sciences and Engineering Division.

[1] P. W. Anderson, Phys. Rev. **109**, 1492 (1958).
[2] B. L. Altshuler and A. G. Aronov, in *Electron-Electron Interactions in Disordered Systems*, edited by M. Pollak and A. L. Efros (North-Holland, Amsterdam, 1985).
[3] P. A. Lee and T. V. Ramakrishnan, Rev. Mod. Phys. **57**, 287 (1985).
[4] B. L. Altshuler, Pis'ma Zh. Eksp. Teor. Fiz. **41**, 530 (1985) [JETP Lett. **41**, 648 (1985)].
[5] P. A. Lee and A. D. Stone, Phys. Rev. Lett. **55**, 1622 (1985).
[6] B. L. Altshuler, A. G. Aronov, A. I. Larkin, and D. E. Khmel'nitskii, Zh. Eksp. Teor. Fiz. **81**, 768 (1981) [Sov. Phys. JETP **54**, 411 (1981)].
[7] B. L. Altshuler, A. G. Aronov, and B. Z. Spivak, Pis'ma Zh. Eksp. Teor. Fiz. **33**, 101 (1981) [JETP Lett. **33**, 94 (1981)].
[8] D. Yu. Sharvin and Yu. V. Sharvin, Pis'ma Zh. Eksp. Teor. Fiz. **34**, 285 (1981) [JETP Lett. **34**, 272 (1981)].
[9] R. A. Webb, S. Washburn, C. P. Umbach, and R. B. Laibowitz, Phys. Rev. Lett. **54**, 2696 (1985).
[10] These oscillations survive disorder averaging unlike those studied by E. N. Bogachek, Fiz. Nizk. Temp. **2**, 473 (1976) Sov. J. Low Temp. Phys. **2**, 235 (1976) for the ballistic systems.
[11] W. A. Little and R. D. Parks, Phys. Rev. Lett. **9**, 9 (1962).
[12] A. V. Khaetskii and B. I. Shklovskii, Zh. Eksp. Teor. Fiz. **85**, 721 (1983) [Sov. Phys. JETP, **58**, 421 (1983).
[13] D. Saint-James and P. G. Gennes, Phys. Lett. **7**, 306 (1963).
[14] E. Ginossar, L. I. Glazman, T. Ojanen, F. von Oppen, W. E. Shanks, A. C. Bleszynski-Jayich, and J. G. E. Harris, Phys. Rev. B **81**, 155448 (2010).
[15] V. M. Galitski and A. I. Larkin, Phys. Rev. B **63**, 174506 (2001)
[16] L. I. Glazman, F. W. J. Hekking, and A. Zyuzin, Phys. Rev. B **46**, 9074 (1992).
[17] A. V. Herzog, P. Xiong, and R. C. Dynes, Phys. Rev. B **58**, 14199 (1998).
[18] U. Patel, Z. L. Xiao, A. Gurevich, S. Avci, J. Hua, R. Divan, U. Welp, and W. K. Kwok, Phys. Rev. B **80**, 012504 (2009).
[19] A. Johansson, G. Sambandamurthy, D. Shahar, N. Jacobson, and R. Tenne, Phys. Rev. Lett. **95**, 116805 (2005).
[20] T. Morgan-Wall, B. Leith, N. Hartman, A. Rahman, and N. Markovic, arXiv:1406.6802.
[21] D. Pekker, G. Refael, and P. M. Goldbart, Phys. Rev. Lett. **107**, 017002 (2011).